

The evolution of the mass-metallicity relation at $z > 3$

R. MAIOLINO⁽¹⁾, T. NAGAO⁽²⁾, A. GRAZIAN⁽¹⁾, F. COCCHIA⁽¹⁾, A. MARCONI⁽³⁾,
 F. MANNUCCI⁽⁴⁾, A. CIMATTI⁽⁶⁾, A. PIPINO⁽⁷⁾, S. BALLERO⁽⁸⁾, A. FONTANA⁽¹⁾,
 G.L. GRANATO⁽⁹⁾, F. MATTEUCCI⁽⁸⁾, G. PASTORINI⁽³⁾, L. PENTERICCI⁽¹⁾, G. RISALITI⁽⁵⁾,
 M. SALVATI⁽⁵⁾, and L. SILVA⁽¹⁰⁾

⁽¹⁾ *INAF - Osservatorio Astronomico di Roma*

⁽²⁾ *National Astronomical Observatory of Japan*

⁽³⁾ *Università di Firenze, Dipartimento di Astronomia*

⁽⁴⁾ *INAF - Istituto di Radioastronomia*

⁽⁵⁾ *INAF - Osservatorio Astrofisico di Arcetri*

⁽⁶⁾ *Università di Bologna, Dipartimento di Astronomia*

⁽⁷⁾ *Astrophysics, University of Oxford*

⁽⁸⁾ *Università di Trieste, Dipartimento di Astronomia*

⁽⁹⁾ *INAF - Osservatorio Astronomico di Padova*

⁽¹⁰⁾ *INAF - Osservatorio Astronomico di Trieste*

Summary. — We present preliminary results of an ESO-VLT large programme (AMAZE) aimed at determining the evolution of the mass-metallicity relation at $z > 3$ by means of deep near-IR spectroscopy. Gas metallicities and stellar masses are measured for an initial sample of nine star forming galaxies at $z \sim 3.3$. When compared with previous surveys, the mass-metallicity relation inferred at $z \sim 3.3$ shows an evolution significantly stronger than observed at lower redshifts. There are also some indications that the metallicity evolution of low mass galaxies is stronger relative to high mass systems, an effect which can be considered as the chemical version of the galaxy downsizing. The mass-metallicity relation observed at $z \sim 3.3$ is difficult to reconcile with the predictions of some hierarchical evolutionary models. We shortly discuss the possible implications of such discrepancies.

PACS 98.62.Ai, 98.62.Bj – .

1. – Introduction

The correlation between galaxy mass and metallicity has been known for a long time [9]. Thanks to the SDSS survey the mass-metallicity relation has been recently confirmed and refined with a sample of more than 50,000 star forming galaxies [15]. The origin of this relation is ascribed to various possible processes. One possibility is that outflows, originated by the starburst winds, are responsible for ejecting enriched gas out of their host galaxies. In low-mass galaxies outflows may exceed the escape velocity, so that

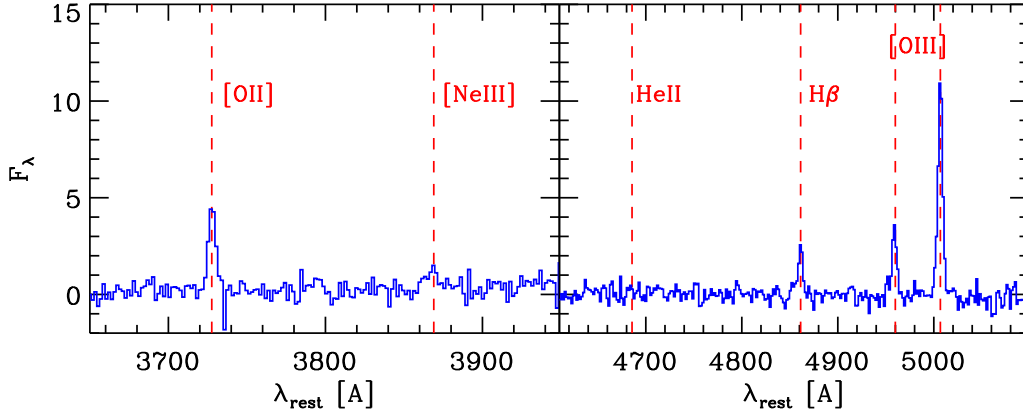


Fig. 1. – Rest frame stacked spectrum of the first nine sources at $3 < z < 3.7$ observed within the AMAZE programme. [OII]3727, [NeIII]3869, H β , [OIII]4959, [OIII]5007 are the nebular lines used to determine the gas metallicity. The expected location of HeII (4686), typically observed in AGNs, is shown to highlight the absence of AGN contribution.

freshly produced metals are lost into the intergalactic medium, therefore yielding a lower effective enrichment; instead, the deeper gravitational potential of massive galaxies is more effective in retaining metals, yielding higher enrichment [15]. Another possibility is that low mass systems are little evolved: they have still to convert most of their gas into stars, and therefore have little enriched their ISM yet; instead, massive systems have converted most of their gas into stars, therefore reaching maturity from the chemical point of view. The latter scenario is commonly referred to as “downsizing”. Finally, it has been proposed that the IMF may change depending on the level of star formation, so that the effective yield of metals is higher during the evolution of galaxies with larger, final stellar masses [7].

The relative role of these different processes in shaping the mass-metallicity relation is debated. However, it is likely that each of them contributes at least to some extent, since observational evidence has been found for each of these processes. Each of these factors (outflows/feedback, downsizing, IMF) has profound implications on the evolution of galaxies. Therefore, it is clear that the mass-metallicity relation contains a wealth of information useful to constrain models of galaxy formation and evolution. Indeed, any model of galaxy evolution is now required to match the mass-metallicity relation observed locally [8, 1, 3]. However, different models predict different evolutionary patterns of the mass-metallicity relation as a function of redshift, and observational data are required to test and discriminate among them. Observational constraints of the mass-metallicity relation have been obtained up to $z \sim 2.2$ thanks to various deep surveys (e.g. [14, 10, 4]). However, at $z > 3$, which is a crucial redshift range as we shall see in the following, the mass-metallicity relation has been little explored yet.

2. – The AMAZE project

We have started a project (AMAZE, Assessing the Mass-Abundance redshift [Z] Evolution) specifically aimed at determining the mass-metallicity relation at $z > 3$. This is an ESO large programme that has been awarded 180 hours of observations with SINFONI,

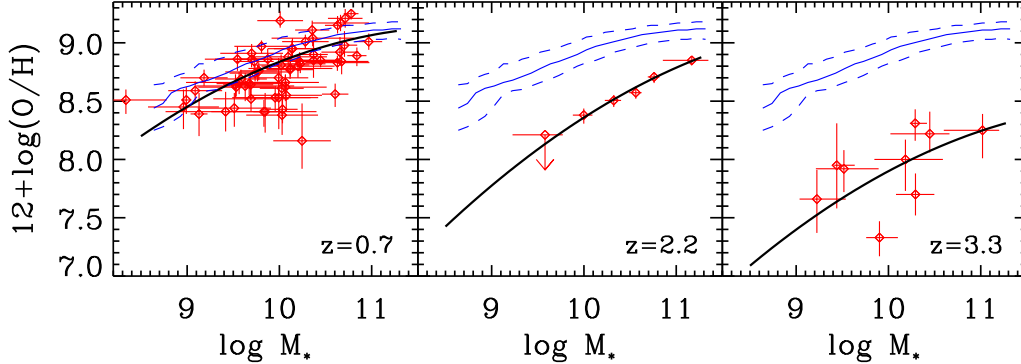


Fig. 2. – Mass-metallicity relation observed at various redshifts (red points with errorbars) compared with the local relation [15] (thin, blue solid and dashed lines). At $z \sim 0.7$ (leftmost panel) we use the data from [14], recalibrated with our relations. At $z \sim 2.2$ (central panel) we use the data from [4] (in this case the data are from stacked spectra and *not* from individual galaxies), also recalibrated with our relations. At $z \sim 3.3$ (rightmost panel) we show the preliminary results for the first nine galaxies in our AMAZE program. Black, solid lines show quadratic fits to the relations at each redshift.

the VLT near-IR integral field spectrometer. The goal is to obtain near-IR spectra of a sample of about 30 galaxies at $3 < z < 5$. At these redshifts the near-IR spectra allow us to measure the fluxes of the nebular emission lines [OII]3727, [NeIII]3869, $H\beta$, [OIII]4959, [OIII]5007, whose relative ratios can be used to constrain the gas metallicity [12]. In particular, by combining all of the diagnostics that can be inferred from these lines [12], we can estimate the gas metallicity by also accounting for the effect of possible dust reddening, and we can also control possible variations of the excitation conditions of the gas (details of this procedure are given in [11]).

The sample has been selected among Lyman Break Galaxies for which Spitzer-IRAC data are available, which are required to obtain a good determination of the stellar mass M_* at $z > 3$ (where the rest-frame near-IR stellar light is redshifted to $\lambda > 3.5 \mu\text{m}$). AGN contamination must be absolutely avoided (since it would affect the line ratios), therefore we also required that the galaxies have hard X-ray and Spitzer-MIPS data: hard X-rays allow us to identify the presence of Compton thin AGNs, while $24 \mu\text{m}$ data allow us to identify even Compton thick AGNs [5, 2].

The observing programme is currently in progress. Here we summarize preliminary results from the first 9 sources at $3 < z < 3.7$ for which spectra have been obtained and reduced (a more detailed discussion of this preliminary set of data is given in [11]). Fig. 1 shows the rest frame, stacked spectrum of these 9 sources, where the nebular lines used to constrain the gas metallicity are indicated. The expected location of HeII (4686), typically observed in AGNs, is shown to highlight the absence of any AGN contribution.

3. – The mass-metallicity relation at $z \sim 3.3$

Fig. 2 (rightmost panel) shows the inferred mass-metallicity relation at $z \sim 3.3$ (red points with errorbars) compared with the local mass-metallicity relation ([15], blue thin lines, adapted to account for the IMF adopted by us). The other panels show the mass-metallicity relation at lower redshifts inferred by using results of previous works [14, 4],

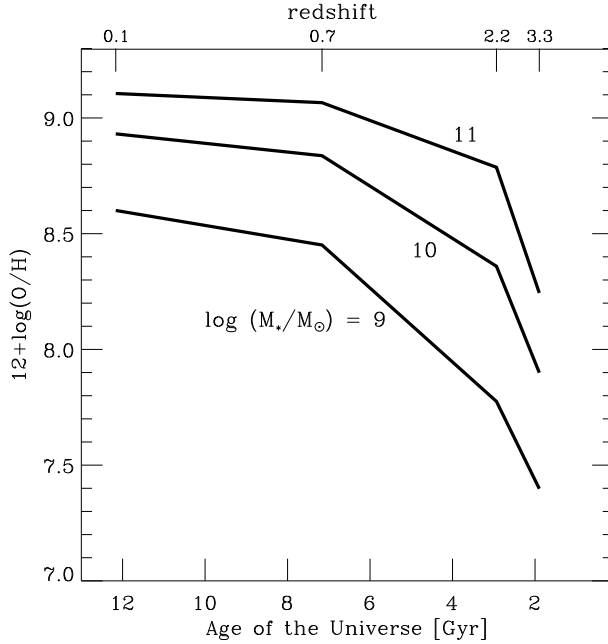


Fig. 3. – Inferred, average metallicity evolution as a function of the age of the universe, for different stellar masses. Note the strong evolution in time between $z=2.2$ and $z=3.3$.

and where metallicities have been re-determined by using the same set of intercalibrated diagnostics adopted by us [12] to ensure consistency between the various methods. Note that at $z\sim 2.2$ the data points are obtained from stacked spectra [4], while at $z\sim 0.7$ and at $z\sim 3.3$ metallicities are inferred from the spectra of individual galaxies. The black, thick solid lines indicate quadratic fits to the data at each epoch.

The mass-metallicity relation evolves significantly from $z=0$ to $z=2$, but only by a factor of about two in metallicity (at high masses), which is not a very strong evolution if one considers that this redshift range embraces 75% of the age of the universe. Between $z=2.2$ and $z=3.3$ the average metallicity decreases by another factor of ~ 3 , but here the temporal evolution is much stronger, since the time elapsed within this redshift range is much shorter. This effect is shown more clearly in Fig. 3, where the evolution of the average metallicity (for different stellar masses) is plotted as a function of the age of the universe. The rate of evolution is clearly steeper at $2.2 < z < 3.3$ than at $z < 2.2$ (especially at high masses), indicating that in the former redshift range we are witnessing an epoch of major action in terms of star formation and of metal enrichment of galaxies.

Figs. 2–3 also suggest that the evolution rate is not constant with mass. At low stellar masses the evolution is stronger than in massive systems. This can be regarded as the chemical version of the galaxy “downsizing”: massive systems reach chemical maturity at higher redshift, while low-mass systems chemically evolve more slowly and over a period of time possibly extending to the present epoch. However, confirming this effect requires more statistics at low masses, where our preliminary mass-metallicity relation is still poorly populated (and possibly more prone to selection effects than massive systems).

When interpreting Figs. 2–3 it is important to bear in mind that at different redshifts surveys are sampling different populations of galaxies. Local star forming galaxies sam-

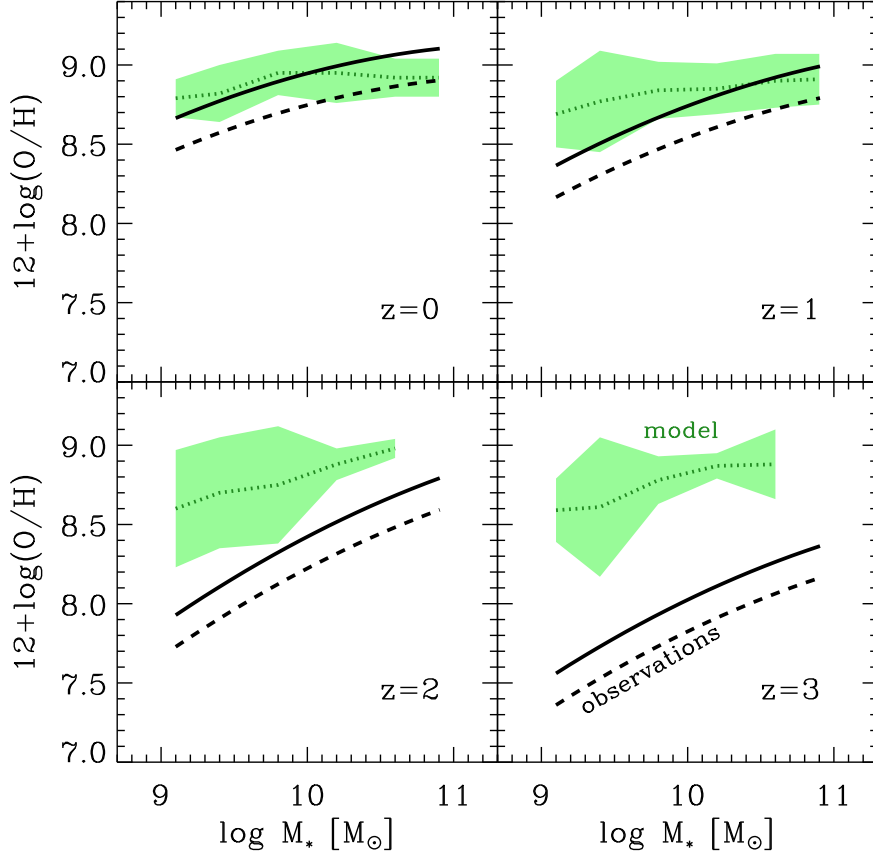


Fig. 4. – Comparison of the evolution of the mass–metallicity relation expected by the hierarchical model in [3] (green, dotted lines and shaded areas) with the evolution measured in the observations (solid, black lines). Observations have been interpolated linearly to match the redshifts available for the theoretical model. The black, dashed lines show the observed mass–metallicity relation shifted by 0.2 dex to account for a possible offset of the metallicity scale [4, 3]. Note the strong discrepancy between the model and observations at $z=3$.

pled by SDSS in [15] are mostly spirals with modest star formation rates, while LBGs used to investigate the mass–metallicity relation at $z \sim 2\text{--}3$ are characterized by enhanced star formation (and will likely evolve into massive, quiescent local galaxies). Therefore, the patterns shown in Figs. 2–3 should not be interpreted as the evolution of individual galaxies, but as the evolution of the average mass–metallicity relation of galaxies representative (or which contribute significantly to) the density of star formation at each epoch. Additional issues related to possible selection effects are discussed in [11].

Within this context it is interesting to note in Fig. 2 the existence of some galaxies at $z \sim 3.3$ with stellar masses approaching $M_* \sim 10^{11} M_\odot$ and metallicity $\sim 0.4 Z_\odot$. According to some models [6, 13], these systems are expected to evolve into very massive ellipticals (approaching $10^{12} M_\odot$) with solar/super-solar metallicities.

4. – Comparison with theoretical models

Fig. 4 shows the comparison between the evolution of the mass-metallicity relation inferred by the observations (black solid lines) and the evolution expected by the simulations within a hierarchical scenario as obtained by [3] (green dotted lines, where shaded areas show the dispersion of the simulations). The dashed lines show the observed mass-metallicity relation with an offset of 0.2 dex, to account for a possible offset in the absolute metallicity scale (see [11, 4] for discussions about this possible issue). While at low redshift there is a fair agreement between model and observations, at high redshift an increasing discrepancy emerges. In particular, at $z \sim 3.3$ observations appears totally inconsistent with the prediction provided by the theoretical model. Similar discrepancies are found by comparing observations with the hierarchical simulations obtained by [8].

The origin of the discrepancy between these hierarchical models and the observations at high redshift is unclear. A possibility is that in these hierarchical models most of the chemical evolution occurs rapidly in small units, at low masses ($M_* < 10^9 M_\odot$). Therefore, according to these models, at high redshift galaxies are mostly assembled with units that are already chemically evolved, yielding a relatively flat relation and relatively high metallicity at $M_* > 10^9 M_\odot$. The lower metallicity found in the observations at $z \sim 3.3$ suggests instead that galaxies at high redshift are made through the assembly of relatively unevolved sub-units. In support of this scenario, we note that the alternative hierarchical models presented in [1] match the mass-metallicity relation at $z \sim 2.2$ much better than the above mentioned models. Indeed, one of the main features of the model in [1] is that a strong feedback prevents sub-units to evolve significantly before merging into more massive systems. Firmer conclusions on the latter class of models require a comparison of the observations with the predictions at $z \sim 3.3$, which are not available in [1] yet.

A more detailed investigation will be possible thanks the completion of the AMAZE project, within about one year.

* * *

We are grateful to S. Savaglio for providing to us the electronic version of the tables in her paper and for useful comments. We also thank A. Brooks for useful discussions. This work was partially supported by INAF and by ASI.

REFERENCES

- [1] BROOKS A.M. ET AL., *ApJ*, **655** (2007) L17.
- [2] DADDI E. ET AL., *ApJ*, **670** (2007) 173.
- [3] DE ROSSI M.E., TISSERA P.B. and SCANNPIECO C., *MNRAS*, **374** (2007) 323.
- [4] ERB D.K. ET AL., *ApJ*, **646** (2006) 107.
- [5] FIORE F. ET AL., *arxiv0705.2864*, (2007) .
- [6] GRANATO G.L. ET AL., *ApJ*, **600** (2004) 580.
- [7] KÖPPEN JM WEIDNER C. and KROUPA P., *ApJ*, **375** (2007) 673.
- [8] KOBAYASHI C., SPRINGEL V. and WHITE S.D.M., *ApJ*, **376** (2007) 1465.
- [9] LEQUEUX J. ET AL., *A&A*, **80** (1979) 155
- [10] LIANG Y.C., HAMMER F. and FLORES H., *A&A*, **447** (2006) 113
- [11] MAIOLINO R. ET AL., *submit.*, (2007)
- [12] NAGAO T., MAIOLINO R., MARCONI A., *A&A*, **459** (2006) 85.
- [13] PIPINO A. ET AL., *ApJ*, **638** (2006) 739.
- [14] SAVAGLIO S. ET AL., *ApJ*, **635** (2005) 260.
- [15] TREMONTI C.A. ET AL., *ApJ*, **613** (2004) 898.